

See discussions, stats, and author profiles for this publication at: <https://www.researchgate.net/publication/231713091>

# Hierarchical Self-Assembly of Epitaxial Semiconductor Nanostructures

ARTICLE *in* NANO LETTERS · NOVEMBER 2004

Impact Factor: 13.59 · DOI: 10.1021/nl048443e

---

CITATIONS

32

---

READS

20

4 AUTHORS, INCLUDING:



Surajit Atha

GE Global Research

11 PUBLICATIONS 146 CITATIONS

SEE PROFILE



Jerrold Floro

University of Virginia

119 PUBLICATIONS 3,352 CITATIONS

SEE PROFILE

# Hierarchical Self-Assembly of Epitaxial Semiconductor Nanostructures

Jennifer L. Gray,<sup>†</sup> Surajit Atha,<sup>†</sup> Robert Hull,<sup>\*,†</sup> and Jerrold A. Floro<sup>‡</sup>

*University of Virginia, Department of Materials Science and Engineering,  
Charlottesville, Virginia 22904, and Sandia National Laboratories, P.O. Box 5800,  
Albuquerque, New Mexico 87185-1415*

*Received September 22, 2004*

## ABSTRACT

We describe a new route to hierarchical assembly of semiconductor nanostructures, employing guided organization of self-assembling epitaxial quantum dot molecules in the  $\text{Ge}_x\text{Si}_{1-x}/\text{Si}(100)$  system. The quantum dot molecule comprises a shallow strain relieving pit, defined by {105} facets, and bounded by 4-fold {105}-faceted islands. Through topographic “forcing functions” fabricated on the substrate surface, the quantum dot molecules may be organized into arrays, enabling hierarchical structures spanning length scales from tens of nanometers to macroscopic dimensions.

We have recently reported the discovery of self-assembling epitaxial quantum dot molecules (QDMs) in the  $\text{Ge}_x\text{Si}_{1-x}/\text{Si}(100)$  system.<sup>1–4</sup> The QDM comprises a shallow strain relieving pit, defined by {105} facets, in the growing  $\text{Ge}_x\text{Si}_{1-x}$  film, and bounded by 4-fold {105}-faceted islands or ridges, and forms under a range of kinetically limited growth conditions. On unpatterned substrates QDMs form at apparently random locations on the growing surface. Here, we show how QDMs may be patterned into ordered arrays using a topographic “forcing function” on the substrate surface, employing arrays of focused ion beam (FIB) fabricated holes of dimensions and spacings that create interstices of appropriate dimensions for QDM formation. The complete array thus comprises a hybrid patterned/self-assembled structure that precisely defines structure at multiple dimensions, from the tens of nanometers length scale of individual quantum dots to the potentially macroscopic dimensions of the topographic forcing function.

The QDM structure is shown in Figures 1a–c. It evolves during molecular beam epitaxy (MBE) growth of  $\text{Ge}_x\text{Si}_{1-x}/\text{Si}(100)$  heterostructures under conditions of limited adatom/ad-dimer mobility, as controlled by combinations of growth temperature and growth rate.<sup>1–4</sup> We illustrate this evolution for growth of  $\text{Ge}_{0.3}\text{Si}_{0.7}$  films at a temperature of 550 °C and a deposition rate of 0.09 nm/s. First, very shallow pits form at a  $\text{Ge}_{0.3}\text{Si}_{0.7}$  film thickness,  $h$ , of 3–5 nm. At  $h \sim 10$  nm, a quadruplet of islands forms at the pit edges, Figure 1a. With subsequent epitaxial growth, these islands extend along the pit perimeters to form a continuous wall by  $h \sim$

20 nm, Figure 1b. During this process, the facet angles of pit and wall progressively increase, until they stabilize at {105}, a strain stabilized surface in Ge and  $\text{Ge}_x\text{Si}_{1-x}$ .<sup>5,6</sup> The QDM size then self-limits,<sup>3</sup> at  $\sim 220$  nm between outer edges of opposite walls, and remains stable during further epitaxial growth until misfit dislocations are injected.<sup>1</sup> This QDM structure has the correct symmetry for potential application to novel nanoelectronic architectures such as quantum cellular automata (QCA),<sup>7,8</sup> where electrons or holes within cells of four quantum dots form bistable states due to Coulomb repulsion, thus representing the two states of digital logic.

Here, we demonstrate that organization of QDMs into large-scale two-dimensional patterns may be achieved using topographic forcing functions fabricated on the Si(001) substrate surface. Arrays of holes were created, ex-situ to the MBE chamber, using an FEI 200 FIB, with a  $\text{Ga}^+$  ion energy of 30 keV and ion current of 11 pA. As-fabricated holes had diameters of 30 nm, depths of 5 or 20 nm, and spacings of 150–750 nm. These patterned surfaces were then cleaned using standard chemical preparation techniques and transferred to a solid-source MBE growth chamber.<sup>1,9</sup> A 36 nm Si buffer was grown at 750 °C, followed by 20 nm of  $\text{Ge}_{0.3}\text{Si}_{0.7}$  growth at 550 °C and a rate of 0.09 nm/s. Figures 2a and 2b show atomic force microscope (AFM) images of the resulting microstructure for a FIB-hole spacing of 250 nm and original hole depth of 5 nm. The FIB holes apparently remain after the substrate cleaning procedure, and morphologically evolve during deposition (this in itself is an interesting process, but not the thrust of this paper). AFM line scans, Figure 2c, show that the depth of the holes following deposition is  $\sim 50$  nm (given the relatively shallow sidewall angle of the holes, the AFM tip should provide a

\* Corresponding author: hull@virginia.edu.

<sup>†</sup> University of Virginia.

<sup>‡</sup> Sandia National Laboratories.

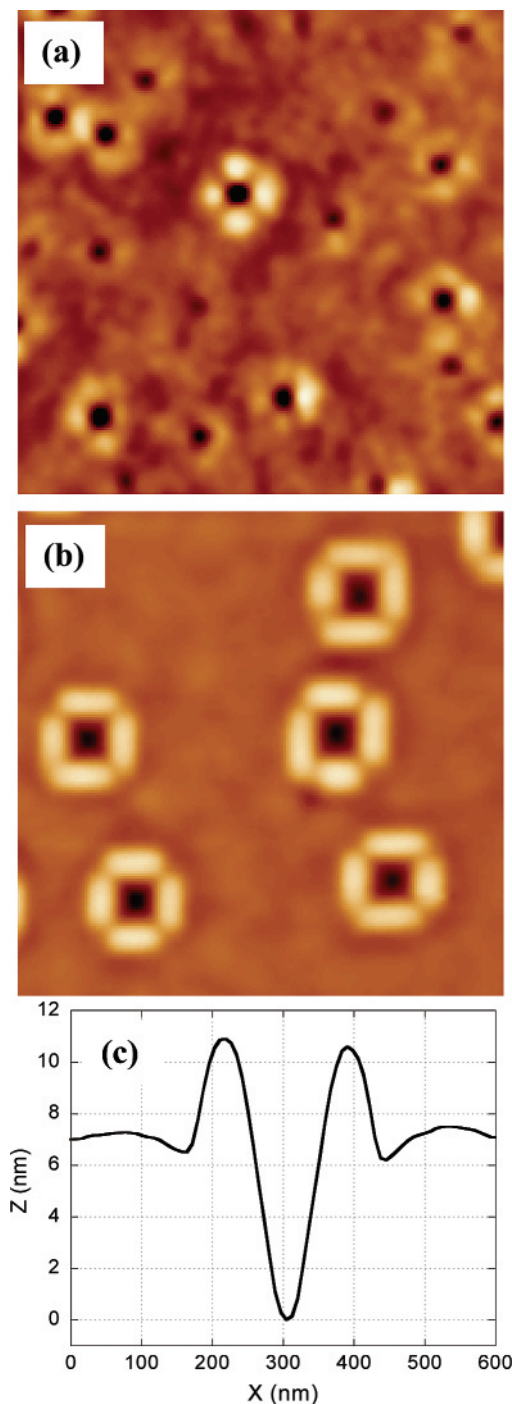


**Figure 1.** AFM images (field of view  $1.0\ \mu\text{m}$ ) of the evolution of the quantum dot molecule for  $\text{Ge}_{0.3}\text{Si}_{0.7}/\text{Si}(100)$  epitaxy at  $550\ ^\circ\text{C}$  and a deposition rate of  $0.09\ \text{nm/s}$ . (a) Intermediate QDM structure (“Compact QDM” or “Quantum Quadruplet”) for  $15\ \text{nm}$  of deposited  $\text{Ge}_{0.3}\text{Si}_{0.7}$ . (b) Final QDM structure (“Mature QDM” or “Quantum Fortress”) for  $20\ \text{nm}$  of deposited  $\text{Ge}_{0.3}\text{Si}_{0.7}$ . (c) Representative AFM linescan from mature QDM structure illustrating the pit/wall geometry.

reasonable estimate of their depth, although a slight under-measurement is possible due to tip-sample geometrical effects), close to the combined depth of the original holes and the deposited films. Within the Si buffer, the hole-sidewall angle is close to a  $\{311\}$  facet, while in the  $\text{Ge}_{0.3}\text{Si}_{0.7}$  film it matches the  $\{105\}$  facet, Figure 2d. Thus, the holes

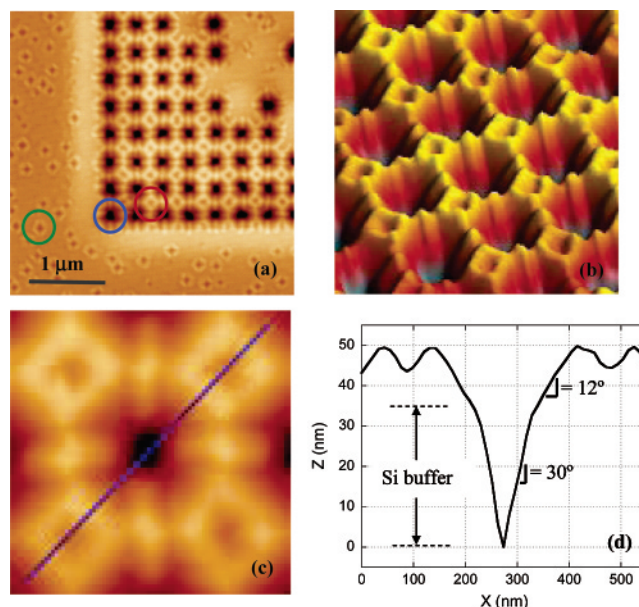


**Figure 2.** AFM images illustrating lithographic ordering of quantum dot molecules for a  $20\ \text{nm}$   $\text{Ge}_{0.3}\text{Si}_{0.7}$  film grown on a patterned  $\text{Si}(100)$  substrate at  $550\ ^\circ\text{C}$  and  $0.09\ \text{nm/s}$ , following deposition of a  $36\ \text{nm}$  Si buffer layer at  $750\ ^\circ\text{C}$ . The patterns were created by  $\text{Ga}^+$  FIB with an ion energy of  $30\ \text{keV}$  and an ion current of  $11\ \text{pA}$ . The as-fabricated features had a diameter of  $30\ \text{nm}$ , a depth of  $5\ \text{nm}$ , and a center-center spacing of  $250\ \text{nm}$ . Figure (a) shows a plan view and Figure (b) a perspective view. In (a), green, red, and blue circles highlight, respectively, a QDM in the unpatterned region, a QDM in the patterned region, and an FIB hole (note region of filled pits in top right of image). (c) Region of AFM line scan across one FIB hole and adjacent QDMs. (d) Topological line scan with facet angles shown for comparison within the Si and  $\text{Ge}_{0.3}\text{Si}_{0.7}$  regions of the FIB-nucleated pits.

have broadened substantially during growth, to about  $100\ \text{nm}$  at the  $\text{Ge}_{0.3}\text{Si}_{0.7}/\text{Si}$  interface and about  $200\ \text{nm}$  at the free  $\text{Ge}_{0.3}\text{Si}_{0.7}$  surface. In the interstices between holes, QDMs form in a regular array, with additional “bridging” quantum dots between interstices. Outside of the patterned region, QDMs form randomly. The dimensions of QDMs inside the patterned array are  $\sim 160\ \text{nm}$ , and outside the array are  $\sim 190\ \text{nm}$  (close to that previously observed on unpatterned  $\text{Si}(001)$  surfaces).<sup>1,3</sup> The interior pits of QDMs in patterned regions are shallower than those in unpatterned regions, with facet angles  $5^\circ$  vs  $9^\circ$ . The average height of the surface between the holes is higher than in the unpatterned regions, consistent with rejection of material from the growing holes during film deposition. Estimates, from AFM images, of the net additional material in the interstice regions with respect to the unpatterned surface are consistent (to within about 20%) with the estimated amount of material rejected from the growing holes.

Retention of the FIB-fabricated holes during the film depositions is key to the patterning of the QDM arrays. We observe that the probability of hole retention depends on the original hole spacing. At spacing  $\leq 200\ \text{nm}$ , Figure 3a, only holes at the periphery of the fabricated pattern are preserved with high probability. As shown in Figure 2a, an original interhole spacing of  $250\ \text{nm}$  allows retention of several layers of holes around the periphery of the pattern, but generally

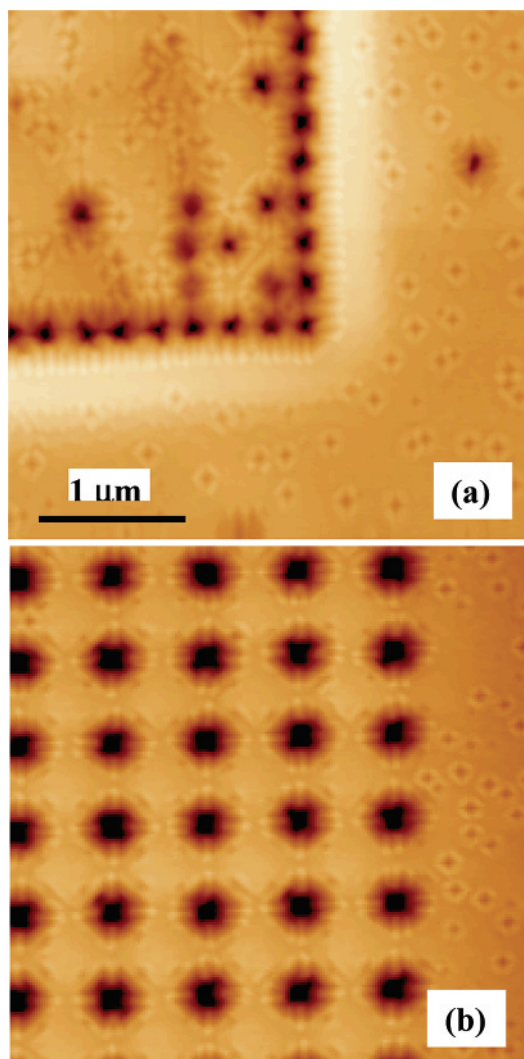


**Figure 3.** AFM images of the effect of the substrate hole spacing upon retention during epitaxial growth, for a 20 nm  $\text{Ge}_{0.3}\text{Si}_{0.7}$  film grown on a patterned Si(100) substrate at 550 °C and 0.09 nm/s, following deposition of a 36 nm Si buffer layer at 750 °C. The initial topographic forcing function is created by an FIB (11 pA current, 30 keV  $\text{Ga}^+$  ions) hole depth of 20 nm and spacings of (a) 200 nm and (b) 500 nm.

not throughout the interior of the pattern (from preliminary results, we observe also at this particular spacing a dependence upon initial hole depth, with greater retention of holes for an as-fabricated depth of 5 nm than for 20 nm). As the spacing increases to 500 nm or greater, Figure 3b, the entire array of holes is retained. These observations are consistent with preferential rejection of deposited material from the growing holes during MBE growth. As hole spacings decrease, the flux of ejected material per unit area of patterned film surface increases. This will produce an effective back flux into adjacent holes, if surface transport lengths under the growth conditions are sufficient for adatoms to migrate between holes. The net rejection of material from the holes is thus reduced, and in the limit of a sufficiently dense array, hole filling would be expected. This premise is supported by the observation that holes in the interior of the arrays tend to fill first, while holes at the periphery are preserved. For these peripheral holes, there is a net flux of

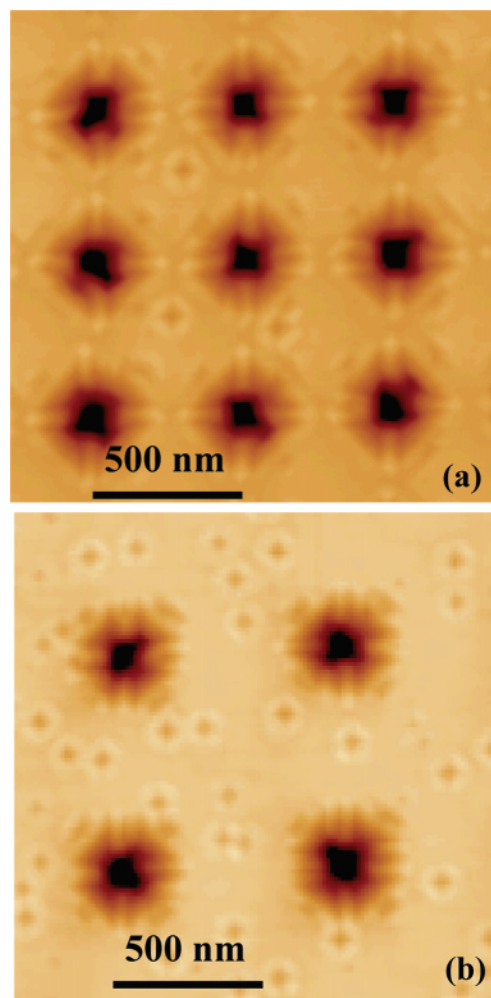


**Figure 4.** AFM images of effect of substrate–hole spacing upon quantum dot organization, for a 20 nm  $\text{Ge}_{0.3}\text{Si}_{0.7}$  film grown on a patterned Si(100) substrate at 550 °C and 0.09 nm/s, following deposition of a 36 nm Si buffer layer at 750 °C. The initial FIB (11 pA current, 30 keV  $\text{Ga}^+$  ions) hole depth is 20 nm and pit spacings are (a) 500 nm and (b) 750 nm.

material out into the unpatterned regions of the film, as evidenced by the regions of higher surface topography at the boundaries of the patterns in Figures 2a and 3. Inspection of the AFM images as a function of hole separation reveals that the transition between filled and unfilled holes in the interior of the array occurs when the surface transport length (as estimated from the width of the raised boundary at the edge of the patterned regions) becomes greater than the hole separation.

In parallel to the need for maintaining the holes during deposition, the dimensions of interstices between holes have to match the QDMs. As discussed above, “mature” (i.e., with a continuous wall of bounding material) QDMs have dimensions  $\sim 220$  nm for growth of  $\text{Ge}_{0.3}\text{Si}_{0.7}$  on unpatterned Si(001) surfaces.<sup>1,3</sup> This “matching” criterion is illustrated by Figure 2a and Figure 4a,b. For hole spacings of 250 nm, Figure 2a, interstices on the final growth surface approximate the unconstrained QDM dimensions and a regular array of QDMs is stabilized on the pattern interstices. For hole spacings of 500 and 750 nm, Figures 4a and 4b, interstices on the final growth surface are substantially larger than the



QDM dimensions and QDM placement is less constrained within the interstices. For the case of  $\text{Ge}_{0.3}\text{Si}_{0.7}$  films studied here, the regimes of pit retention and scaling of interstices to QDM dimensions overlap at an original pit spacing of 250 nm. Further manipulation of these dimensions is possible through the observed inverse scaling of QDM dimensions with strain,<sup>1–4</sup> as previously established for individual  $\text{Ge}_x\text{Si}_{1-x}$  quantum dots on Si.<sup>9–11</sup>

In summary, we have shown that self-assembled epitaxial quantum dot molecules may be ordered through a topographic forcing function encoded into the growth substrate. This finding is significant at several levels. It establishes a route for hierarchical control, at multiple length scales, of self-organizing nanostructures (QDMs) into potentially macroscopic two-dimensional arrays. (These length scales range from the tens of nanometers of individual quantum dots, through the hundreds of nanometers of QDMs, to the dimensions of the topographic forcing function, tens of microns or greater). It provides the potential building blocks for novel nanoelectronic architectures such as QCAs; by appropriate design of the initial hole patterns, circuit elements such as wires, fan-outs, and junctions should be accessible. Finally, it provides a route for demagnification of lithographic patterning, by creating multielement features associated with each lithographic input point.

**Acknowledgment.** This work was funded by NSF-DMR (Grant #0075116) and the NSF-MRSEC “Center for Nano-

scopic Materials Design” at UVa, and by the DOE Office of Basic Energy Sciences. Sandia is a multiprogram laboratory operated by Sandia Corporation, a Lockheed Martin Company, for the United States Department of Energy under Contract No. DE-AC04-94AL85000. We acknowledge useful discussions with J. C. Bean, P. Kumar, and T. E. Vandervelde at Univ. of Virginia.

## References

- (1) Gray, J. L.; Hull, R.; Floro, J. A. *Appl. Phys. Lett.* **2002**, *81*, 2445–7.
- (2) Hull, R.; Gray, J. L.; Kammler, M.; Atha, S.; Kumar, P.; Vandervelde, T.; Bean, J. C.; Floro, J. A.; Ross, F. M. *Mater. Sci. Eng. B* **2003**, *101*, 1–8.
- (3) Gray, J. L.; Singh, N.; Elzey, D. M.; Hull, R.; Floro, J. A. *Phys. Rev. Lett.* **2004**, *92*, 135504–1–3.
- (4) Vandervelde, T. E.; Kumar, P.; Kobayashi, T.; Gray, J. L.; Pernell, T.; Floro, J. A.; Hull, R.; Bean, J. C. *Appl. Phys. Lett.* **2003**, *83*, 5205–7.
- (5) Mo, Y.-W.; Savage, D. E.; Swartzentruber, B. S.; Lagally, M. G. *Phys. Rev. Lett.* **1990**, *65*, 1020–3.
- (6) Shenoy, V. B.; Ciobanu, C. V.; Freund, L. B. *Appl. Phys. Lett.* **2002**, *81*, 364–6.
- (7) Lent, C. S.; Tougaw, P. D.; Porod, W.; Bernstein, G. H. *Nanotechnology* **1993**, *4*, 49–57.
- (8) Amlani, I.; Orlov, A. O.; Toth, G.; Bernstein, G. H.; Lent, C. S.; Snider, G. L. *Science* **1999**, *284*, 289–291.
- (9) Floro, J. A.; Chason, E.; Freund, L. B.; Twisten, R. D.; Hwang, R. Q.; Lucadamo, G. A. *Phys. Rev. B* **1999**, *59*, 1990–8.
- (10) Tromp, R. M.; Ross, F. M.; Reuter, M. C. *Phys. Rev. Lett.* **2000**, *84*, 4641–4.
- (11) Sutter, P.; Lagally, M. G. *Phys. Rev. Lett.* **2000**, *84*, 4637–40.

NL048443E